Eur. Phys. J. B **48**, 113–124 (2005)
DOI: 10.1140/epjb/e2005-00378-9

THE EUROPEAN PHYSICAL JOURNAL B

Nanotube field and one-dimensional fluctuations of C_{60} molecules in carbon nanotubes

K.H. Michel[1], B. Verberck[1,a], and A.V. Nikolaev[2]

[1] Department of Physics, University of Antwerp, Groenenborgerlaan 171, 2020 Antwerpen, Belgium
[2] Institute of Physical Chemistry of the Russian Academy of Sciences, Leninskii prospekt 31, 117915, Moscow, Russia

Received 24 June 2005 / Received in final form 21 September 2005
Published online 9 December 2005 –

Abstract. C_{60} molecules encapsulated in carbon nanotubes interact by van der Waals forces with the tube walls. The nanotube field leads to orientational confinement of the C_{60} molecules which depends on the nanotube radius. In small tubes with radius $R_T \leq 7$ Å a fivefold symmetry axis of the molecule coincides with the tube axis, the center of mass of the molecule being located on the tube axis. The interaction between C_{60} molecules encapsulated in the nanotube is then described by a O_2-rotor model on a one-dimensional (1-d) liquid chain with coupling between orientational and displacive degrees of freedom but no long-range order. This coupling leads to a temperature-dependent chain contraction. The structure factor of the 1-d liquid is derived. In tubes with larger radius the molecular centers of mass are displaced off the tube axis. The distinction of two groups of peapods with on- and off-axis molecules suggests an explanation of the apparent splitting of A_g modes of C_{60} in nanotubes measured by resonant Raman scattering.

PACS. 61.46.+w Nanoscale materials: clusters, nanoparticles, nanotubes, and nanocrystals – 61.48.+c Fullerenes and fullerene-related materials – 81.05.Tp Fullerenes and related materials

1 Introduction

The discovery of carbon nanotubes (CNTs) by Iijima [1] and the subsequent large-scale synthesis [2] of CNTs has opened wide roads for the synthesis and fundamental studies of new materials and for the application of these materials in nanotechnology. For a review on CNTs, see references [3,4]. By now it has become possible to grow novel one-dimensional (1-d) crystalline structures of atoms and molecules inside nanotubes (for a review, see Ref. [5]). In particular the synthesis [6] of self-assembled chains of C_{60} molecules inside single-walled carbon nanotubes (SWCNT), the so-called peapods $(C_{60})_N$@SWCNT, has led to a unique class of nanoscopic hybrid materials with unusual electronic [7] and structural properties. High-resolution transmission electron microscopy observations on sparsely filled CNT [8] demonstrate the motion of molecules along the tube axis and imply that the interaction between C_{60} and the surrounding nanotube wall is due to weak van der Waals forces and not to chemical bonds. At present it is possible to prepare fullerene encapsulating tubules with high filling rate of C_{60} or other fullerene molecules, thereby obtaining 1-d molecular chains [9] inside the tube.

The controlled elaboration of 1-d atomic or molecular structures inside CNTs is of fundamental interest for the study of one-dimensional solids without long-range order. Hitherto the best investigated 1-d chain structures are in fact subsystems of very anisotropic three-dimensional (3-d) crystals. At sufficiently low temperature (T) weak interactions between chains, mediated by the surrounding crystal, lead to long-range order in the subsystems. A prototype of a 1-d chain without long-range order above a transition temperature $T_c = 120$ K is the mercury chain salt $Hg_{3-\delta}AsF_6$, where chains of Hg cations are intercalated into channels formed by the 3-d lattice of AsF_6^- [10,11]. Similary, in the 1-d conductor tetraphenyldithiapyranylidene iodide an organic matrix separates parallel channels filled with I_3^- anions [12]. Also here, below $T_c = 180$ K, a coupling between chains induces a 3-d ordered state.

On the other hand we expect that peapods $(C_{60})_N$@SWCNT behave as truly 1-d molecular liquids down to much lower temperature, possibly they are the ideal 1-d structures without long-range order. Although long-range order is absent, displacive (i.e. center-of-mass displacements) and orientational (i.e. rotations of the molecules) correlations between C_{60} molecules will lead to 1-d crystal-like behavior. However the study of $(C_{60})_N$@SWCNT as a 1-d system is meaningful only for CNTs with small tube radius $R_T \leq 7$ Å where the centers of mass of the molecules are located on the tube axis. For tubes with a radius $R_T \geq 7$ Å total-energy electronic

[a] e-mail: bart.verberck@ua.ac.be

structure calculations show that the stable center-of-mass position is removed away from the nanotube axis [13]. Similar conclusions are drawn from energy potential calculations on spherical structureless molecules in perfect structureless cylindrical nanotubes [14].

In the following we have formulated an analytical theory which takes into account the confinement of the C_{60} molecules by the nanotube wall and the displacive and orientational interactions between molecules.

The content of the paper is as follows. In the next Section 2 we start from a model of van der Waals forces between the C_{60} molecule and a structureless cylindrical SWCNT. We describe the molecule by a rigid skeleton of interaction centers with icosahedral symmetry. We construct the orientation-dependent energy potential experienced by a single C_{60} molecule encapsulated inside a SWCNT. We draw Mercator maps of the potential which show the variation with molecular orientation. The preferential axial orientation of the C_{60} molecule and its center-of-mass position depend on the radius of the nanotube. While we find 1-d crystal-like behavior in small tubes, the 1-d character is lost in larger tubes. The theory suggests an explanation for resonance Raman scattering results [15,16] which show an apparent splitting of A_g modes. In Section 3 we study the van der Waals interactions between C_{60} molecules inside small nanotubes, thereby taking into account the preferential fivefold axial orientations due to the nanotube field. The potential energy of the interacting molecules is then obtained as a two-dimensional (2-D) rotor model on a 1-d chain. Next (Sect. 4) we study orientational and displacive correlations of the non-rigid rotor model. The coupling of rotational and translational degrees of freedom leads to a chain contraction. Short-range correlations are responsible for characteristic peaks in the displacive structure factor, although long-range order is absent. Conclusions are given in the last Section 5.

2 Nanotube field on a C_{60} molecule

We will investigate the energy potential of a single C_{60} molecule inside a SWCNT due to the interaction of the molecule with the tube wall. As a model of the tube we take a structureless cylinder with radius R_{T} and infinite length. The tube wall is approximated by a smooth surface density σ of carbon atoms, where we take the value $\sigma = 0.38$ Å^{-2} as known from graphite. We justify the use of such a model by the fact that the length of the nanotubes is several orders of magnitudes larger than their diameter. Hence we neglect the caps at each end of the tube. In addition the cylindrical portion of a SWCNT formally consists of a single graphene sheet of sp^2-bonded carbon atoms, rolled to form the cylinder [17]. On the other hand, the C_{60} molecule has a distinctive single and double C–C bond structure. We then expect that the interaction potential between the C_{60} molecule and the nanotube wall for a given nanotube radius is rather insensitive on the discrete atomic structure of the cylindrical nanotube wall. Detailed numerical calculations confirm this conjecture [18].

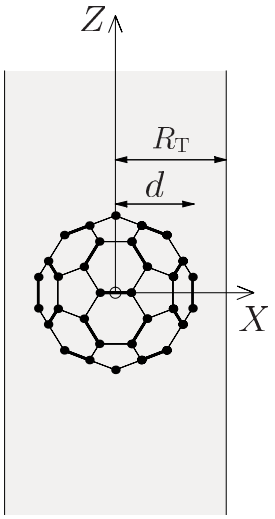

Fig. 1. A C_{60} molecule in standard orientation and in on-axis center-of-mass position in a SWCNT, approximated as a uniform cylinder. Shown is a projection onto the (X, Z) plane. The molecular center of mass is in the coordinate system's origin. The cylinder is aligned along the Z axis.

We consider a tube-fixed Cartesian coordinate system of axes (X, Y, Z) with origin O and such that the Z axis coincides with the axis of the tube. We first study a C_{60} molecule with its center of mass in O, i.e. on the tube axis (also called on-axis position). We recall that the C_{60} molecule, taken as a rigid body, has the shape of a truncated icosahedron (point group symmetry I_h) consisting of 12 pentagons and 20 hexagons [19]. The C–C bonds fusing two hexagons or a hexagon and a pentagon are called double bonds (db) and single bonds (sb) respectively. For a review on properties of fullerenes and fullerene-related compounds, see reference [17]. We consider a molecule-fixed coordinate system of axes (x, y, z) centered in the molecule such that these axes correspond to twofold axes of the molecule. When the molecular system of axes is in coincidence with the tube fixed axes (X, Y, Z), the molecule is said to be in standard orientation (see Fig. 1). The molecule is characterized by a rigid skeleton of interaction centers (ICs) [20,21] located at positions $\{\vec{r}_{\Lambda_i}\}$ on a sphere with radius $d = 3.55$ Å, corresponding to the inner radius of the C_{60} molecule. These centers, labeled by composite indices Λ_i, are of three types $i = 1, 2, 3$: 60 atomic ICs ($i = 1$), a set of 3 ICs on each of the 30 double bonds ($i = 2$) and 60 single-bond ($i = 3$) ICs. The ICs on the molecule interact with the tube wall C-density by van der Waals potentials consisting of a repulsive Born–Mayer part and an attractive London dispersion forces part. The assumption of weak van der Waals forces is supported by the observation of the mobility of the C_{60} molecule along the tube axis in sparsely filled tubes [8]. Also total energy electronic structure calculations show that the interaction of the C_{60} molecule with the tube in the peapod is not due to chemical bonds [22]. For a surface element $d\Sigma(\vec{\rho})$

Table 1. Potential constants C_1, C_2 and B, used for modelling C_{60} – SWCNT and C_{60} – C_{60} interactions, taken from reference [23] except for the value of B^{11} which has been reduced by a factor 0.71. The indices i and $i' = 1, 2, 3$ stand for atomic, double bond and single bond ICs, respectively.

ii'	11	22	33	12	13	23
$C_1^{ii'}$	3.24×10^7 K	1.08×10^6 K	5.92×10^6 K	2.11×10^6 K	6.33×10^6 K	0
$C_2^{ii'}$	3.6 Å^{-1}	3.2 Å^{-1}	3.6 Å^{-1}	3.4 Å^{-1}	3.6 Å^{-1}	0
$B^{ii'}$	4.58×10^5 K Å^6	0	0	0	0	0

around a point $\vec{\rho}$ with cylindrical coordinates (ρ, Φ, Z) on the tube and a center at $\vec{r}_{\Lambda_i}$ on the molecule one has the potential

$$u^i\left(|\vec{\rho} - \vec{r}_{\Lambda_i}|\right) d\Sigma = \sigma\Big\{C_1^{i1} \exp\left[-C_2^{i1}\,|\vec{\rho} - \vec{r}_{\Lambda_i}|\right] - B^{i1}/\,|\vec{\rho} - \vec{r}_{\Lambda_i}|^6\Big\} d\Sigma, \quad (2.1a)$$

where

$$d\Sigma = \rho\delta(\rho - R_{\rm T}) d\rho dZ d\Phi. \quad (2.1b)$$

Here C_1^{i1}, C_2^{i1} and B^{i1} are potential parameters that refer to the interaction of a center of type i with a C-atom ($i' = 1$); we use the potential parameters quoted in Table 1, here and in the following energies are measured in units K (Kelvin).

The positions $\vec{r}_{\Lambda_i}$ are measured in the tube-fixed frame and depend on the orientation of the molecule. We start from the molecule in standard orientation. In terms of tube-fixed spherical coordinates we write $\vec{r}_{\Lambda_i} = (d, \theta_{\Lambda_i}, \phi_{\Lambda_i})$. The total interaction potential between the nanotube and the molecule is called nanotube field potential (subscript NF). With the molecule in standard orientation it reads

$$V_{\rm NF}(R_{\rm T}) = \sigma R_{\rm T} \sum_{i=1}^{3} \sum_{\Lambda_i} \int_0^{2\pi} d\Phi \int_{-\infty}^{+\infty} dZ u^i\left(|\vec{\rho} - \vec{r}_{\Lambda_i}|\right). \quad (2.2)$$

Cylindrical symmetry ($D_{\infty h}$) implies that this interaction does not depend on the azimuthal angles $\{\phi_{\Lambda_i}\}$. It is therefore sufficient to take $\phi_{\Lambda_i} = 0$, and to consider

$$|\vec{\rho} - \vec{r}_{\Lambda_i}| = \Big[(d\sin\theta_{\Lambda_i} - R_{\rm T}\cos\Phi)^2 + (R_{\rm T}\sin\Phi)^2 + (d\cos\theta_{\Lambda_i} - Z)^2\Big]^{\frac{1}{2}}. \quad (2.3)$$

We rewrite $V_{\rm NF}(R_{\rm T})$, as

$$V_{\rm NF}(R_{\rm T}) = \sum_{i=1}^{3} \sum_{\Lambda_i} v^i(R_{\rm T}, \theta_{\Lambda_i}) \quad (2.4a)$$

where

$$v^i(R_{\rm T}, \theta_{\Lambda_i}) = \sigma R_{\rm T} \int_0^{2\pi} d\Phi \int_{-\infty}^{+\infty} dZ u^i\left(|\vec{\rho} - \vec{r}_{\Lambda_i}|\right). \quad (2.4b)$$

Notice that the integrand depends on θ_{Λ_i} and $R_{\rm T}$. Expansion in terms of spherical harmonics yields

$$V_{\rm NF}(R_{\rm T}) = \sum_{i=1}^{3} \sum_{\Lambda_i} \sum_{\substack{l=0 \\ l\ \text{even}}}^{\infty} v_l^i(R_{\rm T}) Y_l^0(\theta_{\Lambda_i}) \quad (2.5)$$

where

$$v_l^i(R_{\rm T}) = 2\pi \int_0^{\pi} Y_l^0(\theta) v^i(R_{\rm T}, \theta) \sin\theta d\theta. \quad (2.6)$$

Rotating the molecule over Euler angles α, β, γ away from its standard orientation we use the transformation law

$$\mathcal{R}(\alpha, \beta, \gamma) Y_l^m(\theta, \phi) = \sum_{n=-l}^{l} \mathcal{D}_{n,m}^l(\alpha, \beta, \gamma) Y_l^n(\theta, \phi). \quad (2.7)$$

Here $\mathcal{R}(\alpha, \beta, \gamma)$ is the rotation operator and $\mathcal{D}_{n,m}^l(\alpha, \beta, \gamma)$ are the Wigner matrices. We adopt the notations and definitions of reference [24]. In the present case, the cylindrical symmetry implies $m = 0$ and hence the Wigner functions $\mathcal{D}_{n,0}^l$ do not depend on the angle α. The nanotube field potential then becomes

$$V_{\rm NF}(R_{\rm T}; \beta, \gamma) = \sum_{i=1}^{3} \sum_{\Lambda_i} \sum_{\substack{l=0 \\ l\text{even}}}^{\infty} \sum_{n=-l}^{l} v_l^i(R_{\rm T}) \mathcal{D}_{n,0}^l(\beta, \gamma) Y_l^n(\theta_{\Lambda_i}, \phi_{\Lambda_i}). \quad (2.8)$$

So far we have exploited the cylinder symmetry, i.e. the site symmetry. The molecular symmetry (I_h) is accounted for by the distribution of interaction centers. We define structure coefficients of the molecule by [21]

$$c_l^{i\,n} = \sum_{\Lambda_i} Y_l^n(\theta_{\Lambda_i}, \phi_{\Lambda_i}). \quad (2.9)$$

It is useful to introduce molecular shape factors

$$g_l^i = \sqrt{\sum_{n=-l}^{l} \left(c_l^{i\,n}\right)^2}, \quad (2.10a)$$

and normalization coefficients

$$\alpha_l^{i\,n} = \frac{c_l^{i\,n}}{g_l^i}. \quad (2.10b)$$

Icosahedral symmetry of the molecule implies that $c_l^{i\,n}$ is different from zero for n even and $l = 0, 6, 10, 12,...$ In addition $\left|\alpha_l^{i\,n}\right|$ does not depend on i, i.e. on the type of the interaction center. One has

$$\alpha_l^{i\,n} = \varepsilon_l^i \alpha_l^{\mathrm{a}\,n}, \tag{2.10c}$$

where $\alpha_l^{\mathrm{a}\,n}$ refer to atomic centers and $\varepsilon_l^i = \pm 1$, see reference [21]. Defining

$$\tilde{g}_l^i = \varepsilon_l^i g_l^i, \tag{2.11}$$

we rewrite the nanotube field potential as

$$V_{\mathrm{NF}}(R_{\mathrm{T}}; \beta, \gamma) = \sum_{l=0,6,10,\ldots} v_l^i(R_{\mathrm{T}}) \tilde{g}_l^i \mathcal{U}_l(\beta, \gamma), \tag{2.12}$$

where

$$\mathcal{U}_l(\beta, \gamma) \equiv \mathcal{U}_l^{\mathrm{a}}(\beta, \gamma) = \sum_{n=-l}^{l} \alpha_l^{\mathrm{a}\,n} \mathcal{D}_{n,0}^l(\beta, \gamma) \tag{2.13}$$

are molecular and cylinder symmetry adapted rotator functions. Rotator functions, originally introduced by James and Keenan [25] are the appropriate variables for the description of orientational-dependent properties of molecules in crystals [26,27]. They incorporate the symmetry of the molecule and the symmetry of the crystal site point group. In the present case the crystal site symmetry is replaced by the $D_{\infty h}$ symmetry of the nanotube.

For a given set of interaction potential parameters, we have plotted the potential $V_{\mathrm{NF}}(R_{\mathrm{T}}; \beta, \gamma)$ for different tube radii in form of Mercator [28] maps as a function of the angles $0 \leq \beta \leq \pi$ and $0 \leq \gamma \leq 2\pi$. Figures 2a and c refer to $R_{\mathrm{T}} = 6.5$ Å and $R_{\mathrm{T}} = 8.5$ Å. In Figure 2a twelve equivalent minima of the potential — which determine the most probable orientations of the molecule — are found. The values ($\beta \approx 58°, \gamma = 0$) correspond to the situation where the molecule has been rotated counterclockwise around the Y axis, away from the standard orientation by an angle $\beta = \arccos 2/(10 + 2\sqrt{5})^{\frac{1}{2}}$. Then, the nanotube's long axis intersects the centers of two opposing pentagons (a fivefold axis of the molecule coincides with the tube axis). The minima correspond to the twelve pentagons on the C_{60} molecule. The twenty maxima appearing in Figure 2a correspond to the energetically unfavorable orientation when the tube axis intersects two opposing hexagon faces (a threefold axis of C_{60} coincides with the tube axis). On the other hand, comparing Figure 2c with Figure 2a, we find that for $R_{\mathrm{T}} = 8.5$ Å, the positions of potential maxima and minima are reversed. Potential minima now correspond to orientations of the molecule where a threefold axis of the molecule coincides with the tube axis. The distinction of two preferred orientations as a function of the tube radius reflects the competition between the short-range repulsive and the long-range attractive parts of the van der Waals interactions. Considering the smaller nanotube with $R_{\mathrm{T}} = 6.5$ Å but neglecting the repulsive interactions, we obtain a Mercator map similar to Figure 2c. For $R_{\mathrm{T}} = 7.5$ Å we find an intermediate case shown in Figure 2b; the competition between repulsive and attractive forces leads to a molecular orientation where a twofold axis of the molecule is parallel to the tube axis. This orientation favors polymerization of C_{60} molecules [29]. We recall that polymerization always occurs in potassium-doped peapods [30].

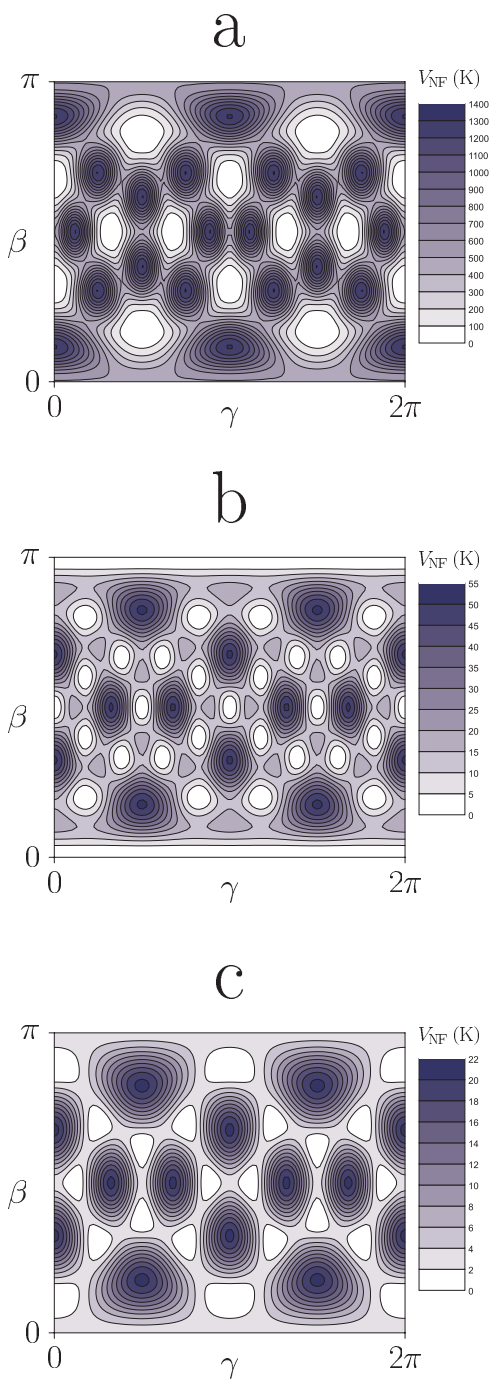

Fig. 2. Mercator maps of the nanotube field potential $V_{\mathrm{NF}}(R_{\mathrm{T}}; \beta, \gamma)$, units K: (a) $R_{\mathrm{T}} = 6.5$ Å, (b) $R_{\mathrm{T}} = 7.5$ Å and (c) $R_{\mathrm{T}} = 8.5$ Å. Center of mass of the C_{60} molecule in on-axis position. The lowest occurring value has been subtracted to make the minimal potential energies lie at zero.

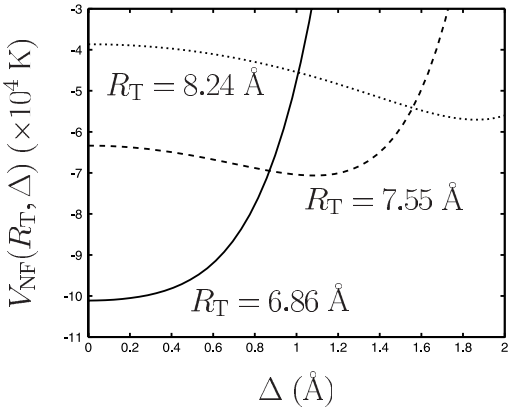

Fig. 3. Variation of the nanotube field potential $V_{\rm NF}(R_{\rm T}, \Delta)$ for three different tube radii: $R_{\rm T} = 6.86$ Å (solid line), $R_{\rm T} = 7.55$ Å (dashed line) and $R_{\rm T} = 8.24$ Å (dotted line), corresponding to $(10, 10)$, $(11, 11)$ and $(12, 12)$ tubes, respectively.

However more important than the change of molecular orientation is the fact that with increasing nanotube radius $R_{\rm T}$, the nanotube axis is no longer a locus of stability for the center of mass of the molecule. In Figure 3 we have plotted the nanotube field potential $V_{\rm NF}(R_{\rm T}, \Delta)$ of the C_{60} molecule with a fivefold axis parallel to the tube axis as a function of the distance Δ of the center of mass of the molecule from the tube axis. For $R_{\rm T} = 7.55$ Å, which corresponds to the radius of an $(11, 11)$ armchair tube [17], the potential difference between the maximum on axis and the minimum off axis at $\Delta_{\rm m} = 1.1$ Å is 5×10^3 K and an order of magnitude larger than any effect of molecular orientation. The displacement of the molecular center-of-mass position away from the nanotube axis for larger tubes reflects the increasing importance of the attractive parts of the van der Waals potential at the expense of the repulsive parts. For C_{60}@$(12, 12)$ with $R_{\rm T} = 8.24$ Å we obtain $\Delta_{\rm m} = 1.8$ Å, comparable to 1.6 Å from total-energy electronic structure calculations [13]. Our results of Figure 3 are in qualitative agreement with potential energy calculations where a homogeneous distribution of C atoms on both the nanotube and the C_{60} molecule was assumed [14]. The large energy differences (order eV) between minima of $V_{\rm NF}(R_{\rm T}, \Delta_{\rm m})$ for $R_{\rm T} \leq 7$ Å, $\Delta_{\rm m} = 0$ and $R_{\rm T} \geq 7$ Å, $\Delta_{\rm m} \neq 0$ respectively, suggests a classification of C_{60}@SWCNT peapods into two groups depending on the tube radius: small nanotubes with molecular center-of-mass positions on-axis and large tubes with off-axis positions.

Resonance Raman scattering [15] measurements on single-walled carbon nanotubes filled with C_{60} molecules exhibit an unexpected splitting of the totally symmetric modes of the C_{60} molecule. In particular, the pentagonal pinch mode $A_g(2)$ "splits" into a doublet $A_g(2)'$ and $A_g(2)''$ below room temperature. This mode, located at 1469 cm^{-1} in pristine C_{60}, can be used as a probe for structural and electronic properties. We attribute the observed splitting of the A_g modes of the C_{60} molecule to two distinct symmetry breakings of the molecule resulting from the on- and off-axis center-of-mass position for small and large nanotubes, respectively. Experiments are carried out on C_{60}@SWCNT with a dispersion of tube radii. This resolves the paradox that there should be no splitting for the non-degenerate A_g modes. The present explanation is corroborated by the experimental fact [15] that thinner tubes tend to yield stronger $A_g(2)''$ components. From Figure 3 we see that the nanotube field potential is larger in absolute value for the smaller than for the larger peapods at their respective molecular center-of-mass positions $\Delta_{\rm m}$.

In line with the present interpretation of the $A_g(2)$ mode "splitting" of C_{60} are conclusions drawn from Raman spectroelectrochemistry experiments [16] on $(C_{60})_N$@SWCNT peapods. The intensity of the mode at 1465 cm^{-1} is considerably increased by anodic doping, in addition there is a satellite line at 1474 cm^{-1}. It is suggested [16] that the satellite line might correspond to peapods of different structure.

Our treatment of the attractive van der Waals forces is based on a summation over attractive pair potentials between interaction centers at $\vec{r}_{\Lambda_i}$ on the molecule and a surface density σ at $\vec{\rho}$ on the nanotube. Assuming London dispersion forces the pair potentials vary with distance as $|\vec{\rho} - \vec{r}_{\Lambda_i}|^{-6}$. By integrating over the nanotube surface, the latter is treated as a macroscopic body. Since the pair potentials are of long range, the result of summation (integration) is not additive but depends on the shape of the macroscopic body. This well-known phenomenon [31] leads to a characteristic inverse power law decrease of the total potential as a function of distance. For instance the attractive interaction energy potential of a neutral atom with a planar dielectric wall at distance L varies as L^{-4}.

Since the nanotube wall has a curvature, we will investigate the inverse power law decrease of the nanotube field with the tube radius $R_{\rm T}$ while keeping the molecule with its center of mass on the tube axis ($\Delta = 0$). We are interested in large values of $R_{\rm T}$, say >20 Å, hence the repulsive Born–Mayer part of the pair potential u^i in equation (2.1a) will become exponentially small, and any relevant contribution to the nanotube field will be due to the attractive part of u^i. To eliminate the dependence of the nanotube field on the orientation of the C_{60} molecule, one should calculate the average crystal field experienced by a C_{60} molecule in a nanotube with radius $R_{\rm T}$,

$$\left\langle V_{\rm NF}(R_{\rm T}) \right\rangle = \frac{1}{2\pi^2} \int_0^{\pi} d\beta \int_0^{2\pi} d\gamma V_{\rm NF}(\beta, \gamma; R_{\rm T}). \quad (2.14)$$

However, for large $R_{\rm T}$, any particular crystal field value $V_{\rm NF}(\beta, \gamma; R_{\rm T})$ is representative since the variation of $V_{\rm NF}$ with (β, γ) decreases rapidly with increasing tube radius $R_{\rm T}$, a trend already observed in Figures 2a–c where the radius is increased from 6.5 Å to 8.5 Å. We have therefore chosen to consider the dependence of $V_{\rm NF}(\beta, \gamma; R_{\rm T})$ on $R_{\rm T}$ at $(\beta, \gamma) = (0, 0)$.

Figure 4 shows the calculated $V_{\rm NF}(0, 0; R_{\rm T}) \equiv V_{\rm NF}(R_{\rm T})$ values for $R_{\rm T}$ ranging from 6 Å till 105 Å with an incremental step of 1 Å. At 7 Å, we observe a minimum; the values at higher $R_{\rm T}$ can be used to determine the long-distance attraction law. We have fitted the data

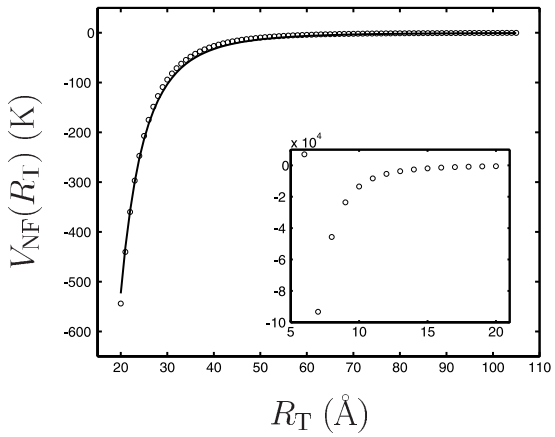

Fig. 4. Calculated values $V_{\rm NF}(\beta = 0, \gamma = 0; R_{\rm T})$ for 20 Å$\leq R_{\rm T} \leq$ 105 Å (dots) and the fitting curve $-c_4/R_{\rm T}^4$ with $c_4 = 8.376 \times 10^7$ K Å^4 (solid line). The Inset shows the $V_{\rm NF}(\beta = 0, \gamma = 0; R_{\rm T})$ values for 6 Å$\leq R_{\rm T} \leq$ 20 Å.

$\big(R_{\rm T}, V_{\rm NF}(R_{\rm T})\big)$ for $R_{\rm T} \geq 20$ Å to attraction laws of the type

$$V_{\rm NF}(R_{\rm T}) = -\frac{c_l}{R_{\rm T}^l}, \tag{2.15}$$

with $l = 3, 4, 5, 6$. From the values of the R^2 goodness-of-fit statistic we conclude that $l = 4$ fits the data best.

3 Intermolecular potentials

Taking advantage of the orientational confinement of the molecules by the encapsulating nanotube, we formulate a 1-d theoretical model of $(C_{60})_N$@SWCNT: beside correlations between center-of-mass positions of the molecules, also orientational correlations have to be taken into account. We will show that at low T, the orientational interaction potential $V^{\rm RR}$ of an individual chain of molecules inside a nanotube corresponds to a O_2-symmetry classical rotor model [32] on a linear chain.

Given the results of the last section, we restrict ourselves to small tubes ($R_{\rm T} \leq 7$ Å) where molecular rotations take place about a fivefold axis which coincides with the Z axis of the nanotube. The corresponding initial axial orientation is shown in Figure 5. Since the nanotube field potential equation (2.12) does not depend on the Euler angle α, an isolated C_{60} molecule can rotate about the Z axis without potential energy change. Following experimental evidence [9], we will study a linear chain of N C_{60} molecules. The molecules are labeled by an index $n \in \mathbb{Z}$, their center-of-mass positions $\{\zeta(n)\}$ are located on the Z axis of the tube. To every C_{60} molecule we assign a rotation angle $\psi(n)$ measuring the rotation about the Z axis away from the initial orientation. We again consider a C_{60} molecule as a cluster of interaction centers; the interaction

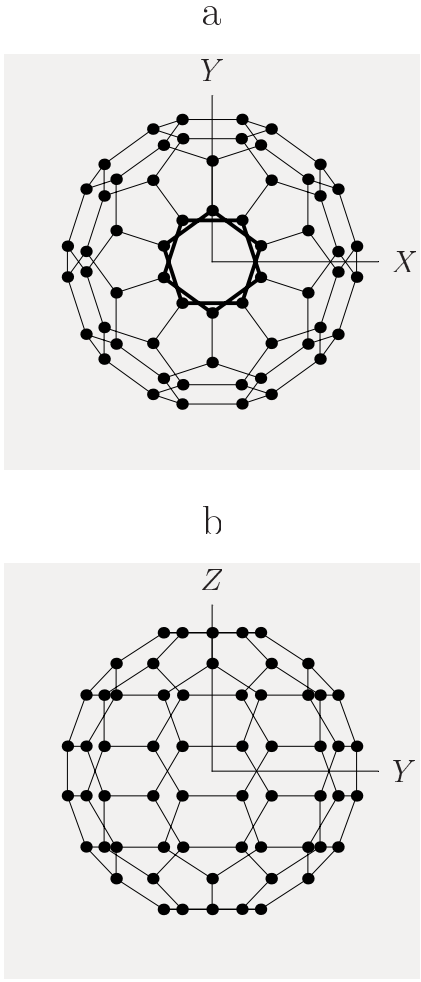

Fig. 5. (a) Projection of a C_{60} molecule, rotated about the Y axis over $\beta \approx 58°$, onto the (X, Y) plane. Note the staggered configuration of the "front" and "back" pentagons, marked bold, and the Z axis being a five-fold symmetry axis. (b) Projection onto the (Y, Z) plane.

energy of two neighboring molecules then reads

$$V^{(2)}(n, n+1) = \sum_i \sum_{i'} \sum_{\Lambda_i} \sum_{\Lambda'_{i'}} U^{ii'}\big(|\vec{r}_{\Lambda_i}(n) - \vec{r}_{\Lambda'_{i'}}(n+1)|\big), \tag{3.1}$$

with the van der Waals pair interaction potential between centers given by

$$U^{ii'}(r) = C_1^{ii'} e^{-C_2^{ii'} r} - \frac{B^{ii'}}{r^6}. \tag{3.2}$$

Here again the potential parameters of Table 1 have been used. The interaction potential equation (3.1) of two confined nearest-neighbor molecules taken as rigid bodies depends on the mutual orientations and on the distance between their centers of mass:

$$V^{(2)}\left(\zeta(n), \zeta(n-1); \psi(n), \psi(n-1)\right) \equiv V^{(2)}\left(\zeta(n) - \zeta(n-1); \psi(n) - \psi(n-1)\right). \tag{3.3}$$

The total interaction potential of N molecules inside the nanotube reads

$$V = \sum_{n=2}^{N} V^{(2)}\left(\zeta(n) - \zeta(n-1); \psi(n) - \psi(n-1)\right). \quad (3.4)$$

Since N is large we will neglect boundary effects.

We first study the rotational interaction of a rigid chain, where all distances $\{\zeta(n) - \zeta(n-1)\}$ are replaced by an average separation a. We write

$$V^{(2)}\left(a; \psi(n) - \psi(n-1)\right) \equiv V^{(2)}\left(\psi(n) - \psi(n-1)\right). \quad (3.5)$$

Taking into account the fivefold rotation symmetry we expand into a Fourier series:

$$V^{(2)}\left(\psi(n) - \psi(n-1)\right) = \sum_{l=0}^{\infty} A_l \cos\left(l\left[\psi(n) - \psi(n-1)\right]\right), \quad (3.6a)$$

where

$$A_l = N_l \int_0^{2\pi} d\psi \cos(l\psi) V^{(2)}(\psi), \quad (3.6b)$$

with $N_0 = (2\pi)^{-1}$ and $N_{l\neq 0} = \pi$. No sine-term ocurs in the expansion (3.6a) since $V^{(2)}(\psi) = V^{(2)}(-\psi)$. Fivefold symmetry implies that the values of l are restricted to $l = 0, 5, 10, \ldots$. Omitting the constant A_0 term in equation (3.6a) and retaining the lowest-order contribution A_5, we obtain

$$V^{(2)}\left(\psi(n) - \psi(n+1)\right) = J\cos\left(5\left[\psi(n) - \psi(n-1)\right]\right) \quad (3.7)$$

where J stands for A_5. Introducing two-dimensional (2-D) vectors

$$\vec{S}(n) = \begin{pmatrix} \cos\left(5\psi(n)\right) \\ \sin\left(5\psi(n)\right) \end{pmatrix} \quad (3.8)$$

as orientational order parameters, we obtain the total rotational interaction contribution V^{RR} from equation (3.4) in the form

$$V^{\mathrm{RR}} = \sum_{n=2}^{N} J\vec{S}(n) \cdot \vec{S}(n-1). \quad (3.9)$$

This expression corresponds to the "Hamiltonian" of a rotor model with O_2 symmetry [32] on a 1-d lattice. With the potential constants of Table 1 we obtain $J = -19$ K < 0. If the two neighboring molecules n and $n-1$ have the same orientation, i.e. $\psi(n) = \psi(n-1)$, then $\vec{S}(n) \cdot \vec{S}(n-1) = 1$, their interaction energy has the minimum value $-|J|$. Recalling that the C_{60} molecule has a center of inversion symmetry (see Fig. 5), we realize that a same axial orientation of two neighboring molecules corresponds to the situation where their two nearest-neighbor pentagonal faces are in staggered configuration, such that the intermolecular repulsion is minimized.

We now will include the actual center-of-mass distances $\zeta(n) - \zeta(n-1)$ and study the coupling of orientational and translational degrees of freedom. Although there is no long-range translational order in the 1-d chain, we may assume that due to short-range correlations the deviations of $\zeta(n) - \zeta(n-1)$ from the average distance a are small and consider

$$\xi(n) = \zeta(n) - \zeta(n-1) - a \quad (3.10)$$

as expansion parameter. Up to second order in $\xi(n)$ we obtain from the right-hand-side (r.h.s.) term of equation (3.4):

$$\begin{aligned} V^{(2)}\left(\zeta(n) - \zeta(n-1); \psi(n) - \psi(n-1)\right) = \\ V^{(2)}\left(\psi(n) - \psi(n-1)\right) + V^{(2)'}\left(\psi(n) - \psi(n-1)\right)\xi(n) \\ + \frac{1}{2} V^{(2)''}\left(\psi(n) - \psi(n-1)\right)\xi(n)^2 + \ldots \end{aligned} \quad (3.11)$$

Here the first term on the r.h.s. is the rigid-lattice term equation (3.5) while $V^{(2)'}$ and $V^{(2)''}$ stand for the first and second derivatives of $V^{(2)}$ with respect to $[\zeta(n) - \zeta(n-1)]$, then taken at $\zeta(n) - \zeta(n-1) = a$. These coefficients still depend on the axial molecular orientation. The expansion in terms of angular coordinates for the rigid lattice term has already been given in equations (3.6a)–(3.9). In addition we now have

$$\begin{aligned} V^{(2)'}\left(\psi(n) - \psi(n-1)\right) = \\ A_0' + A_5' \cos\left(5\left[\psi(n) - \psi(n-1)\right]\right) + \ldots \end{aligned} \quad (3.12)$$

and

$$V^{(2)''}\left(\psi(n) - \psi(n-1)\right) = A_0'' + \ldots \quad (3.13)$$

where

$$A_0' = \frac{1}{2\pi} \int_0^{2\pi} d\psi \left.\frac{\partial V^{(2)}\left(\zeta(n) - \zeta(n-1); \psi\right)}{\partial \zeta(n)}\right|_{\xi(n)=0}, \quad (3.14a)$$

$$A_l' = \frac{1}{\pi} \int_0^{2\pi} d\psi \cos(l\psi) \left.\frac{\partial V^{(2)}\left(\zeta(n) - \zeta(n-1); \psi\right)}{\partial \zeta(n)}\right|_{\xi(n)=0}, \quad (3.14b)$$

$$A_0'' = \frac{1}{2\pi} \int_0^{2\pi} d\psi \left.\frac{\partial^2 V^{(2)}\left(\zeta(n) - \zeta(n-1); \psi\right)}{\partial \zeta(n)^2}\right|_{\xi(n)=0}. \quad (3.14c)$$

The equilibrium lattice constant a is determined by the condition

$$A_0'(a) = 0. \quad (3.15)$$

The calculated value $a = 10.211$ Å is close to the experimental result $a \sim 10$ Å [33]. Restricting ourselves to $l = 0$

and $l = 5$ angular terms, we obtain for the translation- and rotation-dependent potential V, equation (3.4):

$$V = (N-1)A_0 + V^{\mathrm{RR}} + V^{\mathrm{TT}} + V^{\mathrm{RRT}}. \tag{3.16}$$

Here the translation-translation (TT) contribution reads

$$V^{\mathrm{TT}} = \frac{f}{2}\sum_{n=2}^{N}\xi(n)^2, \tag{3.17}$$

where $f = A_0''$ is the lattice "spring constant". The last term V^{RRT} in equation (3.16) accounts for the coupling between translational and rotational degrees of freedom of neighboring C_{60} molecules in the nanotube and reads

$$V^{\mathrm{RRT}} = \lambda\sum_{n=2}^{N}\vec{S}(n)\cdot\vec{S}(n-1)\xi(n). \tag{3.18}$$

Here the coupling constant $\lambda = A_5'$ is obtained from equation (3.14b). Numerical values, resulting from the intermolecular van der Waals potential (3.1), are $f = 18255\ \mathrm{K\,\AA^{-2}}$ and $\lambda = 79\ \mathrm{K\,\AA^{-1}}$. In C_{60} fullerite the interaction V^{RRT} drives [34] the contraction of the crystal lattice [35,36] at the first-order phase transition from the orientationally disordered cubic phase $Fm\overline{3}\mathrm{m}$ to the ordered cubic pahse $Pa\overline{3}$. The interaction V^{RRT} is reminiscent of the spin-lattice interaction in compressible magnets [37] where it leads to phenomena known as magneto-thermomechanics. In the next section we will show that the interaction V^{RRT} leads to a decrease of the average molecular nearest-neighbor distance a with decreasing temperature.

In deriving the orientation-dependent contributions to V, we have taken into account the interaction of the molecule with the nanotube by restricting the orientational degrees of freedom of the molecule to rotations about a fivefold molecular axis which coincides with the tube axis. Once this condition, required for nanotubes with small radii ($R_{\mathrm{T}} \leq 7$ Å), has been imposed, there is no restriction on the molecular rotation angle ψ. This fact is a consequence of our model of a structureless nanotube. On the other hand the question arises whether the situations of nanotubes with armchair (ν,ν) or zig-zag $(\nu,0)$ structure is markedly different if the symmetry of the nanotube is compatible with the symmetry of the fivefold rotation axis of the molecule. Here and in the following we use the notation (ν,μ) where the integers ν and μ are the indices [38,39] which characterize the structure of the nanotube. In case of armchair or zig-zag nanotubes, a "crystal field" potential of the form

$$V_\nu^R = \sum_n A_\nu\cos\big(\nu\psi(n)\big), \tag{3.19}$$

has to be added to the total potential V. Here $\nu = 5p$, where p is a nonzero integer. The amplitude A_ν is a Fourier expansion coefficient of the interaction potential of the molecule with the armchair or zig-zag nanotube wall. The case $p = 1$ corresponds to a coupling of the nanotube wall to the orientational order parameter component $\cos\big(5\psi(n)\big)$. However, the radius of the $(5,5)$ nanotube with value $R_{\mathrm{T}} = 3.43$ Å is too small to allow the encapsulation of a C_{60} molecule with effective outer radius ≈5 Å; the same remark applies to the $(5,0)$ nanotube of even smaller radius. More realistic for C_{60} peapods [33] is the case $p = 2$, referring to the nanotube $(10,10)$ with $R_{\mathrm{T}} = 6.86$ Å. However the corresponding nanotube field which is proportional to $\cos(10\psi)$ does not induce any long-range orientational order since the thermal expectation values $\langle\cos(5\psi)\rangle$ and $\langle\sin(5\psi)\rangle$ vanish. The same result holds for armchair and zig-zag nanotubes with higher indices ν.

The present considerations on 1-d aspects of C_{60} peapods are meaningful for nanotubes with $R_{\mathrm{T}} \leq 7$ Å. For tubes with larger radii, zig-zag and helical chain structures of C_{60} molecules become possible [40,41].

4 Orientational and translational correlations

Although a 1-d model described by the interaction potential (3.16) does not lead to perfect long-range order at finite temperature T we obtain orientational correlations which can interfere with the translational modes. In the following we will calculate correlation functions within classical physics. Due to the large mass and moment of inertia of the C_{60} molecule such an approach is well justified even for T as low as 0.01 K. Nearest-neighbor orientational order parameter correlations, given by the thermal averages

$$\Gamma(1) = \langle\vec{S}(n)\cdot\vec{S}(n-1)\rangle = \langle\cos\left(5\left[\psi(n)-\psi(n-1)\right]\right)\rangle, \tag{4.1}$$

can be evaluated analytically as follows. We define $\phi(n) = 5\left[\psi(n)-\psi(n-1)\right]$, and rewrite the rotational interaction on a rigid lattice as

$$V^{\mathrm{RR}} = \sum_{n=2}^{N} J\cos\phi(n). \tag{4.2}$$

We then calculate

$$\Gamma(1) = \frac{\displaystyle\prod_{n=2}^{N}\int_0^{2\pi} d\phi(n)\cos\phi(n)e^{-V^{\mathrm{RR}}(\{\phi\})/T}}{\displaystyle\prod_{n=2}^{N}\int_0^{2\pi} d\phi(n)e^{-V^{\mathrm{RR}}(\{\phi\})/T}} \tag{4.3}$$

with the result

$$\Gamma(1) = \frac{I_1\left(\frac{|J|}{T}\right)}{I_0\left(\frac{|J|}{T}\right)} \tag{4.4}$$

which is known from the 2-D rotor model [42]. Here we use units $k_{\mathrm{B}} = 1$, i.e. all energies are measured in units K. The functions I_1 and I_0 are modified Bessel functions. This expression approaches the value 0 in the high-T limit and 1 in the low-T limit. The total energy decrease due to

nearest-neighbor orientational correlations of the chain of N molecules is given by

$$\langle V^{\mathrm{RR}}\rangle = -(N-1)|J|\Gamma(1). \tag{4.5}$$

We next turn to translational correlations. A harmonic interaction potential V^{TT} similar to equation (3.17) has been introduced previously [11] for an individual chain of Hg ions in $Hg_{3-\delta}AsF_6$. The mean-square deviation σ^2 in the relative center-of-mass positions of neighboring molecules is obtained from

$$\langle \xi^2(n)\rangle = \frac{\displaystyle\int_{-\infty}^{+\infty} d\xi(2)\ldots\int_{-\infty}^{+\infty} d\xi(N)\xi^2(n)e^{-V^{\mathrm{TT}}/T}}{\displaystyle\int_{-\infty}^{+\infty} d\xi(2)\ldots\int_{-\infty}^{+\infty} d\xi(N)e^{-V^{\mathrm{TT}}/T}} \tag{4.6}$$

with the result

$$\sigma^2 \equiv \langle[\zeta(n)-\zeta(n-1)-a]^2\rangle = \frac{T}{f}. \tag{4.7}$$

While the harmonic potential V^{TT} does not affect the average distance between nearest-neighbor molecules, i.e. $\langle\zeta(n)-\zeta(n-1)\rangle - a = 0$, the coupling V^{RRT} between rotational and translational degrees of freedom leads to a decrease of the average distance. In absence of long-range orientational order at finite temperature, we average V^{RRT} over the orientational degrees of freedom, thereby taking into account short-range correlations:

$$V^{\mathrm{RRT}}(\{\xi(n)\}) = \lambda\Gamma(1)\sum_{n=2}^{N}\xi(n). \tag{4.8}$$

Here the factor $\lambda\Gamma(1) \equiv K$ can be considered as an internal force coupling to the relative center-of-mass displacements. Taking into account V^{RRT} given by equation (4.8) and V^{TT} defined by equation (3.17), we calculate the translational part of the partition function:

$$\begin{aligned} Z &= \frac{1}{a^{N-1}} \\ &\times \int_{-\infty}^{+\infty} d\xi(2)\ldots\int_{-\infty}^{+\infty} d\xi(N)\xi^2(n)e^{\frac{-f}{2T}\sum_n \xi(n)^2 - \frac{K}{T}\sum_n \xi(n)} \\ &= \left(\frac{2\pi T}{a^2 f}\right)^{\frac{N-1}{2}} e^{\frac{(N-1)K^2}{2fT}}. \end{aligned} \tag{4.9}$$

The free energy is given by

$$F = -T\ln Z = C - (N-1)\frac{K^2}{2f}, \tag{4.10}$$

with $C = -(N-1)\frac{T}{2}\ln\frac{2\pi T}{a^2 f}$. Taking the derivative of F with respect to the internal force K we obtain the average center-of-mass distance between nearest-neighbor molecules

$$\langle\zeta(n)-\zeta(n-1)\rangle = a - \lambda\Gamma(1)/f, \tag{4.11}$$

with the static orientational order parameter correlation function $\Gamma(1)$ given by equation (4.4). Since λ, $\Gamma(1)$ and f are positive, the RRT coupling always leads to a reduction of the average distance a between nearest neighbor molecules. For $T = 300$ K, we find a contraction by 0.00014 Å. Since $\Gamma(1)$ increases with decreasing T, the lattice contraction increases with decreasing T; for $T = 10$ K, the contraction becomes 0.0029 Å. In analogy with magneto-thermo-mechanics we call this contraction a phenomenon of torsio-thermo-mechanics.

Although the 1-d model described here does not exhibit translational long-range order, i.e. there are no ideal Bragg peaks in the neutron or X-ray scattering law, we will apply concepts introduced for the description of $Hg_{3-\delta}AsF_6$ [11,43] and show that the structure factor has characteristic resonances in reciprocal space. The static translational structure factor of a non-rigid 1-d chain of N C_{60} molecules with center-of-mass positions $\zeta(n)$ is defined by

$$S(q) = \frac{1}{N}\left\langle\sum_{n=1}^{N}\sum_{n'=1}^{N} e^{-iq[\zeta(n)-\zeta(n')]}\right\rangle. \tag{4.12}$$

Here the wave vector q refers to the momentum transfer $\hbar q$ between the molecules of the chain and the scattered particle (neutron, photon, electron). The thermal expectation value will be calculated with the potential V averaged over the orientational degrees of freedom. Dropping then irrelevant constant terms, we retain

$$V\Big(\{\xi(n)\}\Big) = V^{\mathrm{TT}} + V^{\mathrm{RRT}}\Big(\{\xi(n)\}\Big). \tag{4.13}$$

The calculation of the structure factor is performed in Appendix A, with the result

$$S(q) = \frac{1-Z^2(q)}{1+Z^2(q)-2Z(q)\cos\Big(q\big\langle\zeta(n)-\zeta(n-1)\big\rangle\Big)}. \tag{4.14}$$

Here $Z(q)$ stands for

$$Z(q) = e^{-q^2\sigma^2/2}, \tag{4.15}$$

and $\big\langle\zeta(n)-\zeta(n-1)\big\rangle$, given by equation (4.11), is the average center-of-mass distance between nearest-neighbor molecules in presence of orientational correlations. An expression similar to (4.14) was originally derived by Axe and Emery [11] for a chain of mercury atoms in $Hg_{3-\delta}AsF_6$. The essence is that short-range displacive correlations are systematically taken into account. The present result which applies to $(C_{60})_N$@SWCNT is an extension in as far as it takes into account the axial orientations of the C_{60} molecules as well as the coupling of molecular displacements to orientational correlations. In Figure 6 we have plotted $S(q)$ for $T = 300$ K. The translational structure factor exhibits narrow peaks centered around

$$q_j = j\frac{2\pi}{\big\langle\zeta(n)-\zeta(n-1)\big\rangle}, \tag{4.16}$$

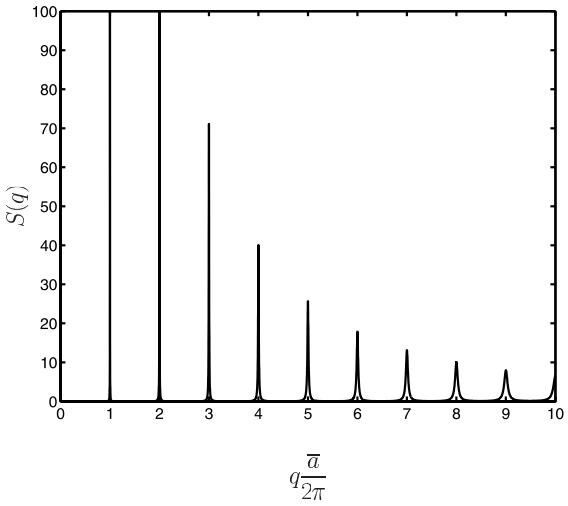

Fig. 6. Structure factor $S(q)$ at $T = 300$ K, abscissa $\overline{q} = q\frac{\langle\zeta(n)-\zeta(n-1)\rangle}{2\pi}$.

$j \in \mathbb{Z}$. These peaks give rise to thin sheets in reciprocal space. They appear as streaks in the experimental diffraction pattern [9].

5 Conclusions

In peapods $(C_{60})_N$@SWCNT the nanotube field potential is the analogue of the crystal field in molecular crystals. Starting from a model of van der Waals interaction potentials between a C_{60} molecule and the cylindrical wall of the surrounding SWCNT, we have formulated the nanotube field potential as a function of nanotube radius R_T and molecular orientations. Thereby we have introduced molecular and cylinder symmetry adapted rotator functions. Drawing Mercator [28] maps (see Figs. 2a–2c) of the nanotube field potential as a function of molecular orientations for a variety of tube radii, we find distinct axial orientations (a symmetry axis of the molecule is parallel to the nanotube axis). For tubes with small radii ($R_T \lesssim 7$ Å), the repulsive part of the van der Waals potential is dominant and a fivefold axis of the molecule coincides with the tube long axis, for larger radii, $R_T \gtrsim 7.9$ Å, the attractive part of the van der Waals potential prevails and a threefold axis of the molecule coincides with the tube axis. For 7 Å$\lesssim R_T \lesssim 7.9$ Å the preferred axial orientation in the nanotube field corresponds to a twofold axis of the C_{60} molecule.

However energetically more important than the change of molecular orientation with increasing tube radius it the fact that for $R_T \gtrsim 7$ Å, the nanotube axis is no longer a locus of stability for the molecular center-of-mass position (Fig. 3). Our results are in agreement with previous theoretical work based on first-principles calculations [13] and on potential energy calculations for spherical molecules in structureless nanotubes [14].

We point out that in a range near 7 Å the C_{60} molecules have their centers of mass on the tube axis with a twofold molecular axis coinciding with the tube axis. This configuration is a prerequisite for polymerisation by cycloaddition of neighboring C_{60} molecules [29,30].

Two distinct molecular center-of-mass positions, on-axis for $R_T \lesssim 7$ Å and off-axis for $R_T \gtrsim 7$ Å, correspond to fields of distinct strength and symmetry experienced by the molecule in small- and large-radii nanotubes. Distinct fields lead to distinct internal mode frequencies of the encapsulated C_{60} molecule. Since experiments are performed on an assembly of nanotubes with a dispersion of radii, the present results on the nanotube field give a convincing explanation of resonant Raman spectroscopy results where one measures an apparent "splitting" of A_g Raman modes [15,16] at sufficient low temperature.

While in C_{60} peapods the dependence of the nanotube field on molecular orientations leads only to weak energy differences, it should be more important for more anisotropic molecules like C_{70}. There a splitting of electron diffraction peaks is interpreted in terms of two distinct orientations of the C_{70} molecule [9]. We expect that the corresponding distinct nanotube fields will also lead to a splitting of A' Raman peaks.

We have studied a linear chain of N interacting C_{60} molecules with fivefold axial orientation in small nanotubes. Since the interaction of two nearest-neighbor molecules depends only on the difference of their orientation angles, we find that the rotational interaction potential corresponds to a O_2 symmetry rotor model. Although there is no true long-range orientational order, interactions between neighboring molecules are attractive and favor orientational correlations. Due to the inversion symmetry of the C_{60} molecules, the neighboring faces of two nearest-neighbor molecules with a same orientation angle are in staggered configuration. Orientational correlations are increasing with decreasing temperature. Taking into account center-of-mass displacements of the molecules along the nanotube axis, we have shown that the coupling of translational and rotational degrees of freedom leads to a shortening of the average intermolecular distance. Even if we do not assume chemical bonds between neighboring molecules, there is an effective attraction due to orientational and displacive correlations which might lead to clustering of groups of neighboring molecules in sparsely filled tubes. These groups would appear as dimers or trimers ..., although there is no true polymerization. We expect that these concepts will be useful for the interpretation of recent inelastic neutron scattering experiments [44] on the dynamics of C_{60} molecules inside nanotubes. Indeed, starting from the O_2 rotor model on a non-rigid chain and taking into account the coupling of translational and orientational degrees of freedom, we are planning to calculate dynamic correlation functions.

Taking into account orientational and translational correlations, we have calculated the translational structure factor, thereby extending previous work [11] on 1-d fluctuations and chain ordering in $Hg_{3-\delta}AsF_6$. In the future these concepts should be incorporated in a more unified theory on the structure of peapods [45] and nanotubes [46].

The authors thank P. Launois and D. Lamoen for useful discussions. The present work has been supported by the Bijzonder Onderzoeksfonds, Universiteit Antwerpen (BOF – NOI). B.V. is a research assistant of the Fonds voor Wetenschappelijk Onderzoek – Vlaanderen.

Appendix A

Here we will give details on the calculation of the structure factor $S(q)$. Starting from the definition equation (4.12), we rewrite the distances $\zeta(n) - \zeta(n')$ in terms of deviations from average nearest-neighbor distances by means of relation (3.10). For $n = n' + m$ we have

$$\zeta(n'+m) - \zeta(n') = \xi(n'+m) + \ldots + \xi(n'+1) + ma. \tag{A.1}$$

We then obtain

$$S(q) = 1 + \left(1 - \frac{1}{N}\right)\left[e^{-iqa}R(q) + e^{iqa}R(-q)\right] + \left(1 - \frac{2}{N}\right)\left[e^{-2iqa}R^2(q) + e^{2iqa}R^2(-q)\right] + \ldots \tag{A.2}$$

with thermal averages $R(\pm q) = \langle e^{\mp iq\xi}\rangle$ given by

$$R(\pm q) = \frac{\displaystyle\int_{-\infty}^{\infty} d\xi e^{\mp iq\xi} e^{-U(\xi)/T}}{\displaystyle\int_{-\infty}^{\infty} d\xi e^{-U(\xi)/T}}. \tag{A.3}$$

Here $U(\xi)$ stands for

$$U(\xi) = \frac{f}{2}\xi^2 + K\xi \tag{A.4}$$

with $K \equiv \lambda\Gamma(1)$. By integration we obtain

$$R(\pm q) = e^{\mp iq\frac{K}{f}} Z(q), \tag{A.5}$$

where $Z(q)$ is defined by equation (4.15) with $\sigma^2 = T/f$, equation (4.7). We rewrite equation (A.2) as

$$S(q) = 1 + 2\left\{\left(1 - \frac{1}{N}\right)\cos(x)Z(q) + \left(1 - \frac{2}{N}\right)\cos(2x)Z^2(q) + \ldots\right\} \tag{A.6}$$

where

$$x = q\left[a - \frac{K}{f}\right] = q\big\langle\zeta(n) - \zeta(n-1)\big\rangle. \tag{A.7}$$

The last equality is obtained by equation (4.11). We consider the expression within braces for large N, use the fact $Z(q) < 1$ for convergence and apply the identity

$$1 + Z\cos x + Z^2\cos(2x) + \ldots = \frac{1 - Z\cos x}{Z^2 - 2Z\cos x + 1}. \tag{A.8}$$

The structure factor then becomes

$$S(q) = 1 + 2\left\{\frac{Z(q)\cos x - Z^2(q)}{Z^2(q) - 2Z(q)\cos x + 1}\right\}, \tag{A.9}$$

which is equivalent to equation (4.14).

References

1. S. Iijima, Nature (London) **354**, 56 (1991)
2. T.W. Ebbesen, P.M. Ajayan, Nature (London) **358**, 220 (1992)
3. R. Saito, G. Dresselhaus, M.S. Dresselhaus, *Physical Properties of Carbon Nanotubes* (Imperial College Press, London, 1998)
4. P.J.F. Harris, *Carbon Nanotubes and Related Structures* (Cambridge University Press, Cambridge, 1999)
5. J. Sloan, A.I. Kirkland, J.L. Hutchison, M.L.H. Green, Chem. Commun., 1319 (2002)
6. B.W. Smith, M. Monthioux, D.E. Luzzi, Nature (London) **396**, 323 (1998)
7. D.J. Hornbaker, S.J. Kahng, S. Misra, B.W. Smith, A.T. Johnson, E.J. Mele, D.E. Luzzi, A. Yazdani, Science **295**, 829 (2002)
8. B.W. Smith, M. Monthioux, D.E. Luzzi, Chem. Phys. Lett. **315**, 31 (1999)
9. K. Hirahara, S. Bandow, K. Suenaga, H. Kato, T. Okazaki, H. Shinohara, S. Iijima, Phys. Rev. B **64**, 115420 (2001)
10. I.D. Brown, Cutforth B.D., C.G. Davies, R.J. Gillespi, P.R. Ireland, J.E. Vekris, Can. J. Chem. **52**, 791 (1974)
11. V.J. Emery, J.D. Axe, Phys. Rev. Lett. **40**, 1507 (1978)
12. P.A. Albouy, J.P. Pouget, H. Strzelecka, Phys. Rev. B **35**, 173 (1987)
13. S. Okada, M. Otani, A. Oshiyama, Phys. Rev. B **67**, 205411 (2003)
14. M. Hodak, L.A. Girifalco, Phys. Rev. B **68**, 085405 (2003)
15. R. Pfeiffer, H. Kuzmany, T. Pichler, H. Kataura, Y. Achiba, M. Melle-Franco, F. Zerbetto, Phys. Rev. B **69**, 035404 (2004)
16. L. Kavan, L. Dunsch, H. Kataura, Chem. Phys. Lett. **361**, 79 (2002)
17. M.S. Dresselhaus, G. Dresselhaus, P.C. Eklund, *Science of Fullerenes and Carbon Nanotubes* (Academic Press, 1996)
18. B. Verberck, K.H. Michel, unpublished
19. H.W. Kroto, J.R. Heath, S.C. O'Brien, R.F. Curl, R.E. Smalley, Nature (London) **318**, 162 (1985)
20. M. Sprik, A. Cheng, M.L. Klein, J. Phys. Chem. **96**, 2027 (1992)
21. J.R.D. Copley, K.H. Michel, J. Phys.: Condens. Matter **5**, 4353 (1993); D. Lamoen, K.H. Michel, Z. Phys. B **92**, 323 (1993)
22. S. Okada, S. Saito, A. Oshiyama, Phys. Rev. Lett. **86**, 3835 (2001); A. Rochefort, Phys. Rev. B **67**, 115401 (2003)
23. B. Verberck, K.H. Michel, A.V. Nikolaev, J. Chem. Phys. **116**, 10462 (2002)
24. C.J. Bradley, A.P. Cracknell, *The Mathematical Theory of Symmetry in Solids* (Clarendon, Oxford, 1972)
25. H.M. James, T.A. Keenan, J. Chem. Phys. **31**, 12 (1959)
26. M. Yvinec, R.M. Pick, J. Phys. France **41**, 1045 (1980)
27. K.H. Michel, K. Parlinski, Phys. Rev. B **31**, 1823 (1985)
28. Gerardus Mercator (1512–1594), Flemish cartographer, inventor of the cylindrical projection

29. A. Trave, F.J. Ribeiro, S.G. Louie, M.L. Cohen, Phys. Rev. B **70**, 205418 (2004)
30. T. Pichler, H. Kuzmany, H. Kataura, Y. Achiba, Phys. Rev. Lett. **87**, 267401 (2001)
31. See e.g. L.D. Landau und E.M. Lifschitz, *Lehrbuch der Theoretischen Physik IX, Statistische Physik, Teil 2*, Kapitel VIII, p. 335 (Akademie-Verlag Berlin, 1984)
32. P.M. Chaikin, T.C. Lubensky, *Principles of Condensed Matter Physics* (Cambridge University Press, Cambridge, 1995), Chapter 6
33. B. Burteaux, A. Claye, B.W. Smith, M. Monthioux, D.E. Luzzi, J.E. Fischer, Chem. Phys. Lett. **310**, 21 (1999)
34. D. Lamoen, K.H. Michel, Phys. Rev. B **48**, 807 (1993)
35. W.I.F. David, R.M. Ibberson, T.J.S. Dennis, J.P. Hare, K. Prassides, Europhys. Lett. **18**, 219 (1992); W.I.F. David, R.M. Ibberson, T.J.S. Dennis, J.P. Hare, K. Prassides, Europhys. Lett. **18**, 735 (addendum)
36. P.A. Heiney, G.B.M. Vaughan, J.E. Fischer, N. Coustel, D.E. Cox, J.R.D. Copley, D.A. Neumann, W.A. Kamitakahara, K.M. Creegan, D.M. Cox, J.P. McCauley, Jr., A.B. Smith III, Phys. Rev. B **45**, 4544 (1992)
37. H. Wagner, Phys. Rev. Lett. **25**, 31 (1970)
38. N. Hamada, S. Sawada, A. Oshiyama, Phys. Rev. Lett. **68**, 1579 (1992)
39. R.A. Jishi, M.S. Dresselhaus, G. Dresselhaus, Phys. Rev. B **47**, 16671 (1993)
40. M. Hodak, L.A. Girifalco, Phys. Rev. B **67**, 075419 (2003); A. Khlobystov, D.A. Britz, A. Ardavan, G.A.D. Briggs, Phys. Rev. Lett. **92**, 245507 (2004)
41. K.S. Troche, V.R. Coluci, S.F. Braga, D.D. Chinellato, F. Sato, S.B. Legoas, R. Rurali, D.S. Galvao, Nano Lett. **5**, 349 (2005)
42. H.E. Stanley, *Phase Transitions and Critical Phenomena* (Clarendon, Oxford, 1971)
43. R. Spal, C.E. Chen, T. Egami, P.J. Nigrey, A.J. Heeger, Phys. Rev. B **21**, 3110 (1980)
44. J. Cambedouzou, S. Rols, R. Almairac, J.L. Sauvajol, H. Kataura, H. Schober, Phys. Rev. B **71**, 041403(R) (2005)
45. J. Cambedouzou, V. Pichot, S. Rols, P. Launois, P. Petit, R. Klement, H. Kataura, R. Almairac, Eur. Phys. J. B **42**, 31 (2004)
46. S. Amelinckx, A. Lucas, P. Lambin, Rep. Progr. Phys. **62**, 1471 (1999)